A novel multigrid approach for solving incompressible Navier-Stokes equations on massively parallel supercomputers

Yu. Feldman and A. Gelfgat

School of Mechanical Engineering
Faculty of Engineering
Tel-Aviv University

Outline

- Concept and motivation
- Pressure-velocity coupled formulation of the Navier-Stokes equations
- Benchmark problems
- Analytical Solution Accelerated (ASA) smoother
- 3D domain decomposition and scalability properties
- Application to the linear stability analysis
- Conclusions

Target: *Incompressible Navier-Stokes equations*

Continuity: $$\nabla \cdot \boldsymbol{u} = 0$$

Momentum: $$\frac{\partial \boldsymbol{u}}{\partial t} + (\boldsymbol{u} \cdot \nabla)\boldsymbol{u} = -\nabla p + \frac{1}{Re}\nabla^2 \boldsymbol{u}$$

- No separate equation for pressure
- No boundary conditions for pressure
- Assume: no simplifications possible

Concept: *Fixed structured grid + Pressure-velocity linked formulation*

Curved boundaries on fixed grid:

Immersed boundary approach (Peskin, 1977)

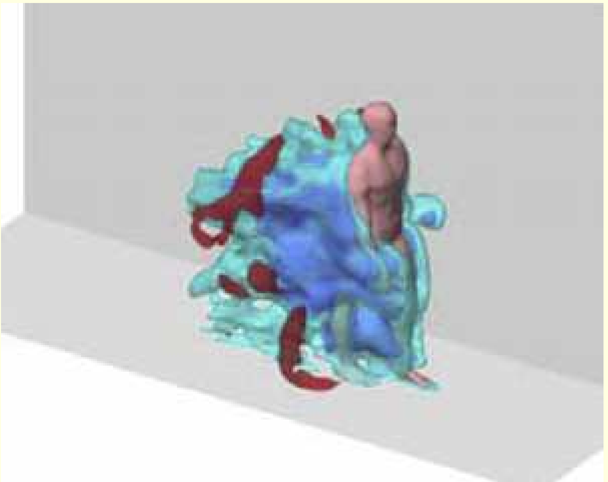

Choi et al., 2007

Moving boundaries on fixed grid:

Volume-of-Fluid (Hirt & Nichols, 1981) or **Level Set** (Osher, 1988) methods

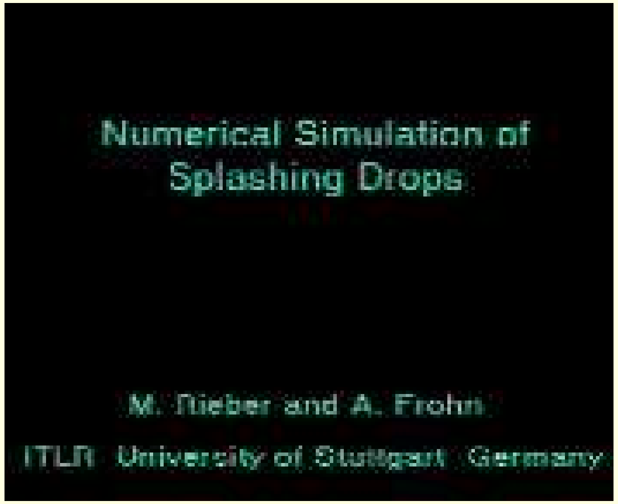

Why not to decouple pressure and velocity ?

Pressure-velocity decoupling:

- ✓ Good robustness
- ✓ Low memory consumption
- ✘ Slow rate of convergence
- ✘ Non-physical pressure field
- ✘ Not applicable for liquid – solid interface problems

Pressure-velocity coupling:

- ✓ Better convergence
- ✓ This is what the nature asks for
- ✓ The obtained pressure is physical
- ✘ High memory consumption
- ✘ Not as robust as decoupling methods

Benchmark Problems

Lid-driven cubic cavity

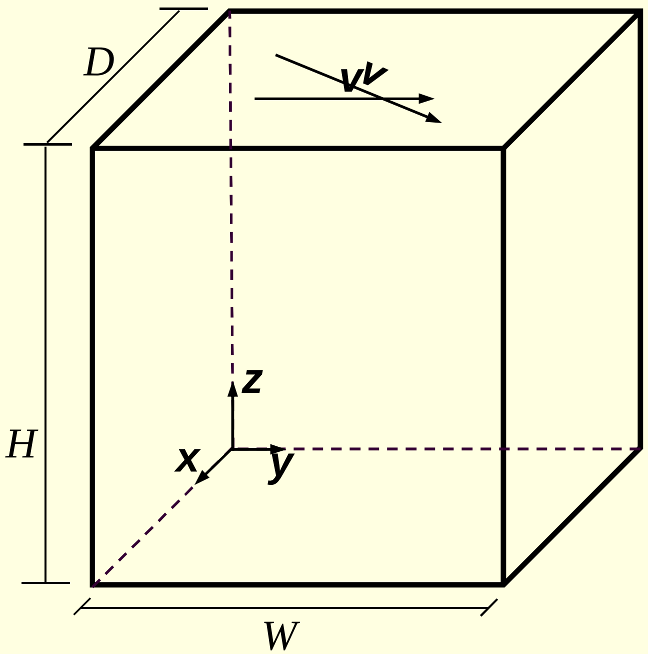

Differentially heated cubic cavity

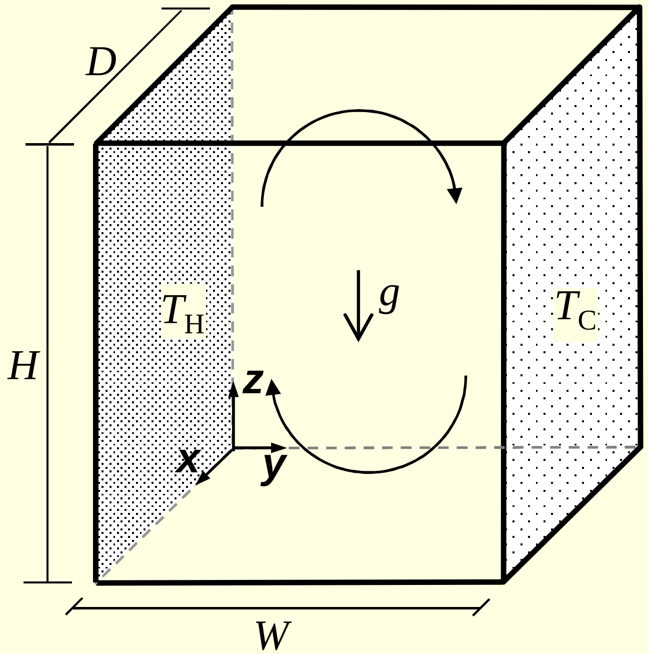

Staggered grid for finite volume method

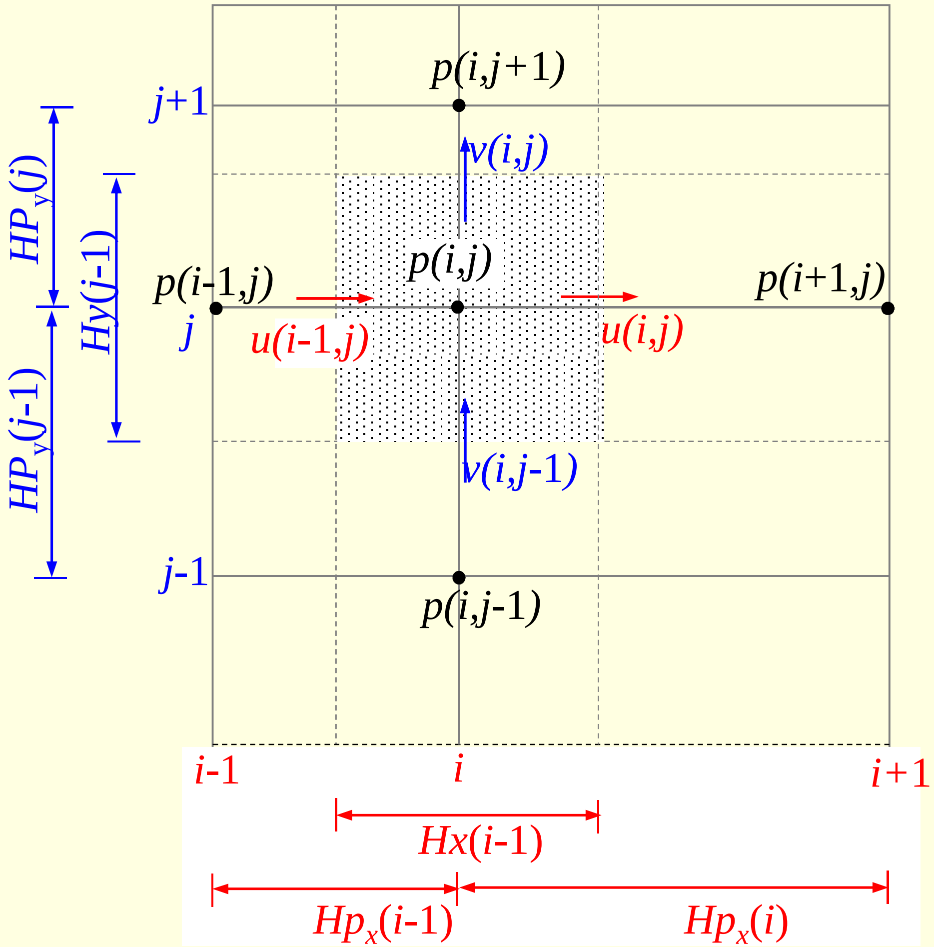

The target: *efficient time-stepping*

To perform a time step <=> inverse of the *Stokes operator*

$$\begin{bmatrix} \frac{1}{\Delta t} - \frac{\Delta^{(u)}}{Re} & 0 & 0 & \partial_x \\ 0 & \frac{1}{\Delta t} - \frac{\Delta^{(v)}}{Re} & 0 & \partial_y \\ 0 & 0 & \frac{1}{\Delta t} - \frac{\Delta^{(w)}}{Re} & \partial_z \\ \partial_x & \partial_y & \partial_z & 0 \end{bmatrix} \begin{pmatrix} u \\ v \\ w \\ p \end{pmatrix} = \begin{pmatrix} f_u \\ f_v \\ f_w \\ 0 \end{pmatrix}$$

+ *boundary conditions for velocity*

+ *Dirichlet point for pressure*

Stokes operator

Multigrid approach **–** a possible choice

✓Low memory and CPU time consumption, *O(N)*

✓ Pressure-velocity coupling can be utilized

✓ Easily parallelized (by MPI or Open MP tools)

✘ Non-constant convergence rate

✘ Sophisticated programming is needed

Multigrid approach – the concept

Typical Multigrid Cycle – Correction Scheme (CS)

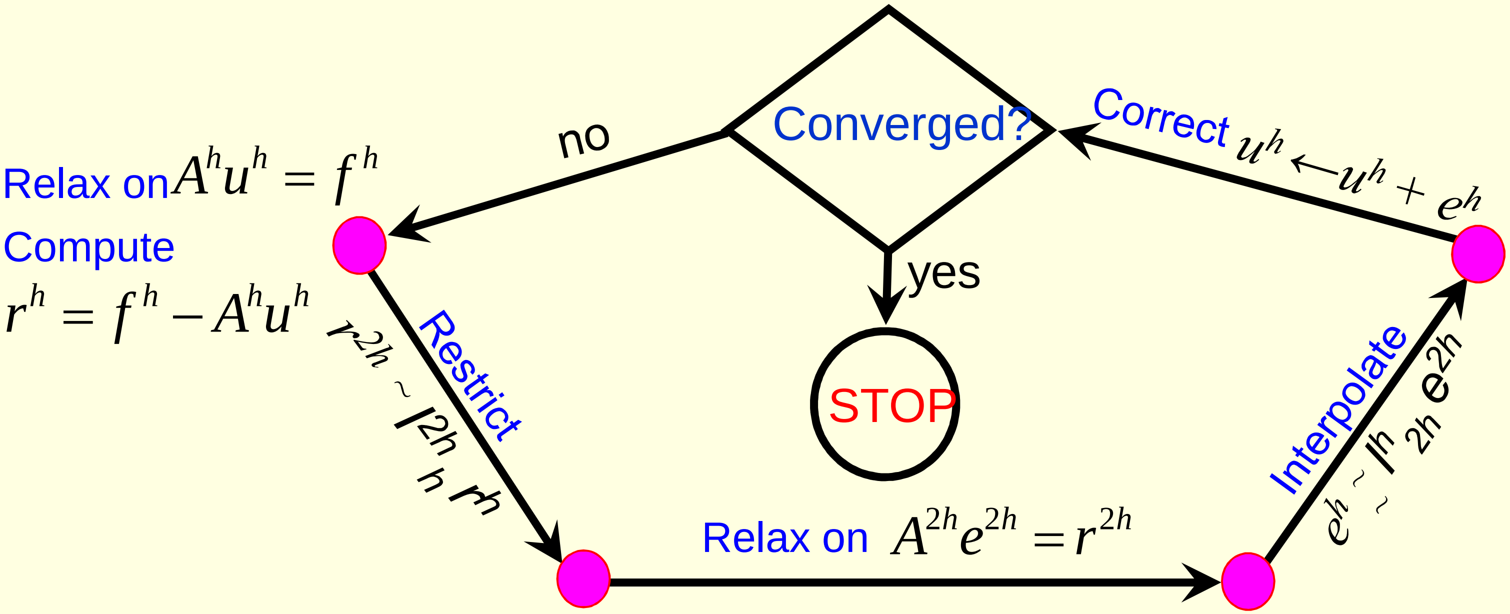

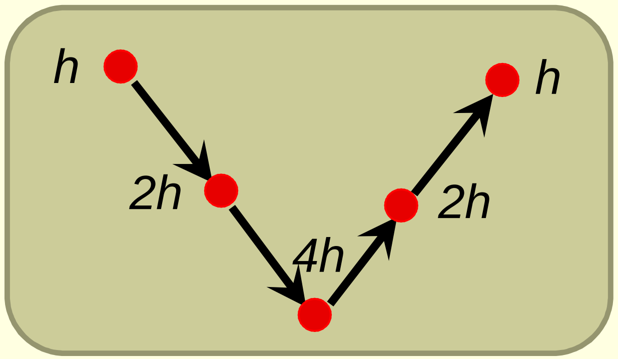

V - cycle

Symmetrical coupled Gauss-Seidel smoothing operator (SCGS)

S.P. Vanka (1985) – analytical solution for a ***single*** finite volume

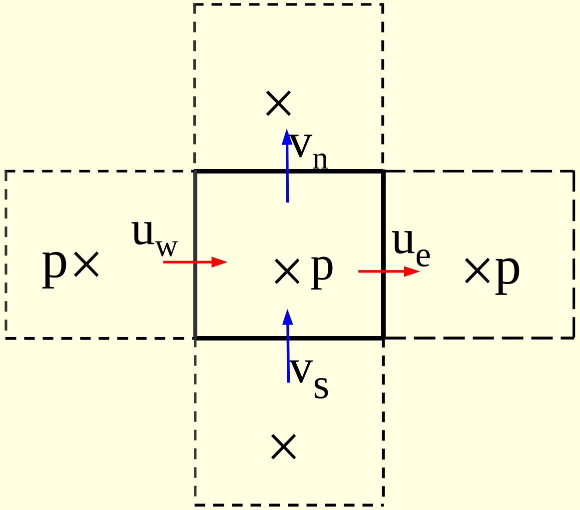

$$(u,v)^{\text{new}} = (u,v)^{\text{old}} + r_{(\text{u,v})}(u,v)'$$

$$p^{\text{new}} = p^{\text{old}} + r_{\text{p}}\,p'$$

$$\begin{bmatrix} A_1 & 0 & 0 & 0 & A_2 \\ 0 & A_3 & 0 & 0 & A_4 \\ 0 & 0 & A_5 & 0 & A_6 \\ 0 & 0 & 0 & A_9 & A_{10} \\ A_7 & -A_7 & A_8 & -A_8 & 0 \end{bmatrix} \times \begin{bmatrix} u'_{\text{e}} \\ u'_{\text{w}} \\ v'_{\text{n}} \\ v'_{\text{s}} \\ p'_{\text{P}} \end{bmatrix} = \begin{bmatrix} R_{\text{ue}} \\ R_{\text{uw}} \\ R_{\text{vn}} \\ R_{\text{vs}} \\ R_{\text{cp}} \end{bmatrix}$$

for the Stokes operator and a constant time step A_i are constants and the 5×5 matrix can be inversed analytically

Accelerated Coupled Line Gauss-Seidel Smoother (ASA-CLGS) -2D

Zeng and Wesseling (1993) – CLGS: Horizontal (vertical) sweeping with horizontally (vertically) adjacent pressure linkage: inverse of block – tri-diagonal matrix for single row (column)

Feldman and Gelfgat (2009) – ASA-CLGS: Horizontal (vertical) sweeping without horizontally (vertically) adjacent pressure linkage: analytical solution over single row (column)

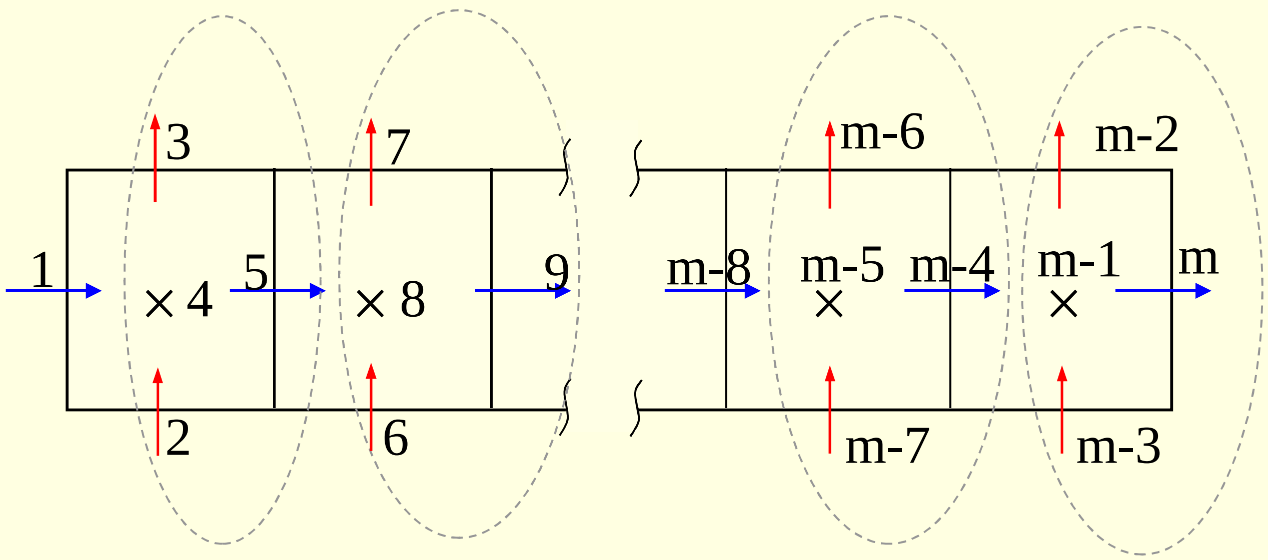

Accelerated coupled line Gauss-Seidel smoother (ASA-CLGS) -2D

Zeng and Wesseling (1993) – CLGS:

$$\cdots$$

$$A^{(x)}_{i+1/2,j}u'_{i+1/2,j}+B^{(x)}_{i+1/2,j}p'_{i,j}=R^{(x)}_{i+1/2,j}$$

$$A^{(x)}_{i-1/2,j}u'_{i-1/2,j}-B^{(x)}_{i-1/2,j}p'_{i,j}=R^{(x)}_{i-1/2,j}$$

$$A^{(y)}_{i,j+1/2}v'_{ij+1/2}-B^{(y)}_{i,j+1/2}\left(p'_{i,j+1}-p'_{i,j}\right)=R^{(y)}_{i,j+1/2}$$

$$A^{(x)}_{i,j}\left(u'_{i+1/2,j}-u'_{i-1/2,j}\right)+A^{(y)}_{i,j}\left(v'_{i,j+1/2}-v'_{i,j-1/2}\right)=0$$

$$\cdots$$

Feldman and Gelfgat (2008) – ASA-CLGS:

$$\cdots$$

$$A^{(x)}_{i+1/2,j}u'_{i+1/2,j}+B^{(x)}_{i+1/2,j}p'_{i,j}=R^{(x)}_{i+1/2,j}$$

$$A^{(x)}_{i-1/2,j}u'_{i-1/2,j}-B^{(x)}_{i-1/2,j}p'_{i,j}=R^{(x)}_{i-1/2,j}$$

$$A^{(y)}_{i,j+1/2}v'_{ij+1/2}+B^{(y)}_{i,j+1/2}p'_{i,j}=\widetilde{R}^{(y)}_{i,j+1/2}$$

$$A^{(x)}_{i,j}\left(u'_{i+1/2,j}-u'_{i-1/2,j}\right)+A^{(y)}_{i,j}\left(v'_{i,j+1/2}-v'_{i,j-1/2}\right)=0$$

$$\cdots$$

where $\widetilde{R}^{(y)}_{i,j+1/2}=R^{(y)}_{i,j+1/2}+B^{(y)}_{i,j+1/2}p'_{i,j+1}$

Analytical solution over a column for ASA-CLGS smoother

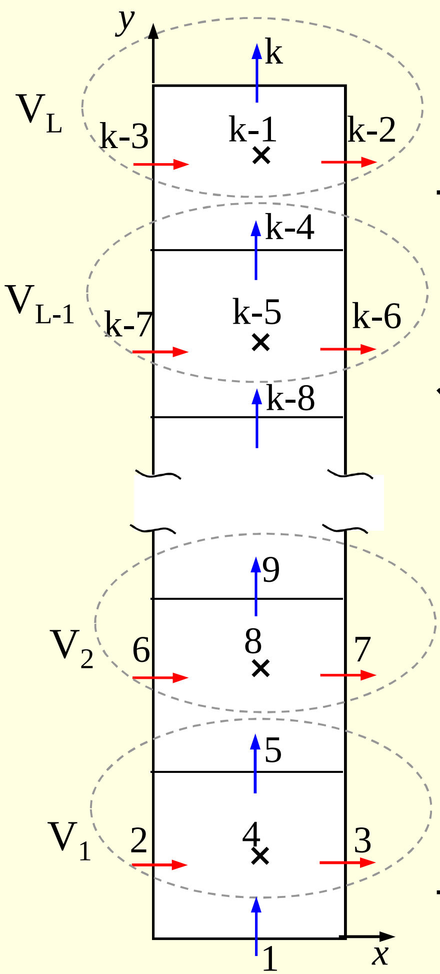

$$\begin{bmatrix} A_1^L & 0 & 0 & 0 & A_2^L \\ 0 & A_3^L & 0 & 0 & A_4^L \\ 0 & 0 & A_5^L & 0 & A_6^L \\ 0 & 0 & 0 & 1 & 0 \\ A_7^L & -A_7^L & A_8^L & -A_8^L & 0 \end{bmatrix} \times \begin{bmatrix} u'_{\text{k-2}} \\ u'_{\text{k-3}} \\ v'_{\text{k}} \\ v'_{\text{k-4}} \\ p'_{\text{k-1}} \end{bmatrix} = \begin{bmatrix} R_{\text{k-2}} \\ R_{\text{k-3}} \\ R_{\text{k}} \\ R_{\text{k-4}} \\ R_{\text{k-1}} \end{bmatrix} \Rightarrow \begin{array}{l} u'_{\text{k-2}} = \alpha_{\text{k-2}}^L p'_{\text{k-1}} + \beta_{k-2}^L \\ u'_{\text{k-3}} = \alpha_{\text{k-3}}^L p'_{\text{k-1}} + \beta_{k-3}^L \\ v'_{\text{k}} = \textit{from b.c.} \\ v'_{\text{k-4}} \ \textit{from volume } L-1 \\ p'_{\text{k-1}} = \alpha_{\text{k-1}}^L v'_{\text{k-4}} + \beta_{k-1}^L \end{array}$$

$$\begin{bmatrix} A_1^I & 0 & 0 & 0 & A_2^I \\ 0 & A_3^I & 0 & 0 & A_4^I \\ 0 & 0 & A_5^I & 0 & A_6^I \\ 0 & 0 & 0 & 1 & 0 \\ A_7^I & -A_7^I & A_8^I & -A_8^I & 0 \end{bmatrix} \times \begin{bmatrix} u'_{\text{m-2}} \\ u'_{\text{m-3}} \\ v'_{\text{m}} \\ v'_{\text{m-4}} \\ p'_{\text{m-1}} \end{bmatrix} = \begin{bmatrix} R_{\text{m-2}} \\ R_{\text{m-3}} \\ R_{\text{m}} \\ R_{\text{m-4}} \\ R_{\text{m-1}} \end{bmatrix} \Rightarrow \begin{array}{l} u'_{\text{m-2}} = \alpha_{\text{m-2}}^L p'_{\text{m-1}} + \beta_{m-2}^L \\ u'_{\text{m-3}} = \alpha_{\text{m-3}}^L p'_{\text{m-1}} + \beta_{m-3}^L \\ v'_{\text{m}} = \alpha_{\text{m}}^L p'_{\text{m-1}} + \beta_{m-4}^L \\ v'_{\text{m-4}} \ \textit{from volume } M-1 \\ p'_{\text{m-1}} = \alpha_{\text{m-1}}^L v'_{\text{m-4}} + \beta_{m-1}^L \end{array}$$

$$\begin{bmatrix} A_1^1 & 0 & 0 & 0 & A_2^1 \\ 0 & A_3^1 & 0 & 0 & A_4^1 \\ 0 & 0 & A_5^1 & 0 & A_6^1 \\ 0 & 0 & 0 & 1 & 0 \\ A_7^1 & -A_7^1 & A_8^1 & -A_8^1 & 0 \end{bmatrix} \times \begin{bmatrix} u'_3 \\ u'_2 \\ v'_5 \\ v'_1 \\ p'_4 \end{bmatrix} = \begin{bmatrix} R_3 \\ R_2 \\ R_5 \\ R_1 \\ R_4 \end{bmatrix} \Rightarrow \begin{array}{l} u'_3 = \alpha_3^L p'_4 + \beta_3^L \\ u'_2 = \alpha_2^L p'_4 + \beta_2^L \\ v'_5 = \alpha_5^L p'_4 + \beta_5^L \\ v'_1 \ \textit{from b.c.} \\ p'_4 = \alpha_4^L v'_1 + \beta_4^L \end{array}$$

CLGS and ASA-CLGS efficiency estimation for 2D

Zeng and Wesseling (1993) – CLGS:

↓

Block 3-diagonal matrix

↓

Block – or 7-diagonal Thomas algorithm

↓

$$\approx O(15M)$$

Feldman and Gelfgat (2009) – ASA-CLGS (6-Diagonal Matrix)

↓

$$p'_{k-1} = (c_1^L v'_{k-4} + R_{k-1}^L + \sum_{i=2}^{4} c_i^L R_{k-i}^L)/c_5^L$$

↓

$$\begin{bmatrix} v'_5 \\ u'_2 \\ u'_3 \end{bmatrix} = \begin{bmatrix} c_6^1 \\ c_7^1 \\ c_8^1 \end{bmatrix} \times p'_4 + \begin{bmatrix} c_9^1 R_5^L \\ c_{10}^1 R_2^L \\ c_{11}^1 R_3^L \end{bmatrix}$$

↓

$$\approx O(5M)$$

↔

Thomas Algorithm (3-Diagonal Matrix)

↓

$$\approx O(5M)$$

ASA-CLGS -efficiency estimation for 3D

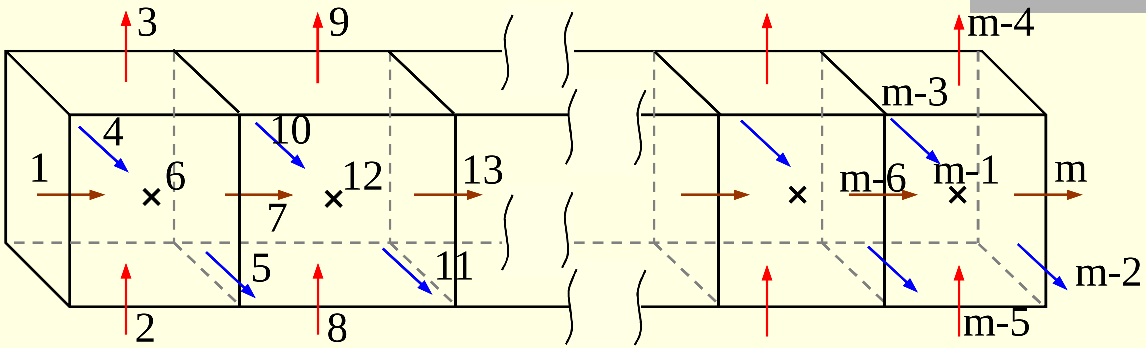

$$p'_p = \left(c_1^I w'_d + R_p^I + c_2^I R_e^I + c_3^I R_w^I + c_4^I R_n^I + c_5^I R_5^I + c_6^I R_d^I\right) / c_7^I$$

$$\begin{bmatrix} w'_d \\ v'_s \\ v'_n \\ u'_w \\ u'_e \end{bmatrix} = \begin{bmatrix} c_8^I \\ c_9^I \\ c_{10}^I \\ c_{11}^I \\ c_{12}^I \end{bmatrix} \times p'_p + \begin{bmatrix} c_{13}^I R_d^I \\ c_{14}^I R_s^I \\ c_{15}^I R_n^I \\ c_{16}^I R_w^I \\ c_{17}^I R_e^I \end{bmatrix}$$

6 corrections for a single volume result in 17 multiplications and divisions and 11 summations

$$\approx O(5M)$$

Advantages and limitations of ASA-CLGS Approach

- ☑ **There exists an analytical solution for the entire corrections row (column).**
- ☑ **Only *O(*5M) operations are needed to obtain the entire row (column) corrections per one sweep for both 2D and 3D geometries**
- ☑ **Effective for stretched grids.**
- ☑ **Effective for flows with a dominating direction**

- ✖ **Up to now applicable only for structured Cartesian grids.**
- ✖ **Slow convergence rate for large time steps**

Domain decomposition for 3D configuration

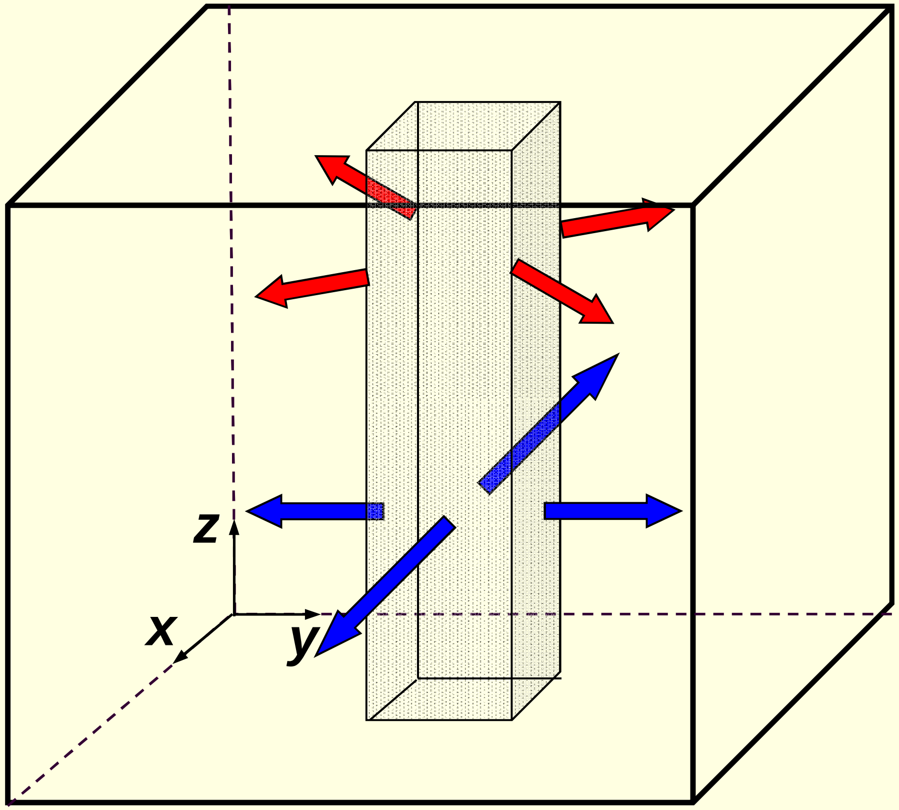

Existence of analytical solution for the whole column allows for 2D virtual topology of 3D configuration.

All volumes located at the sub -volume faces exchange data with neighbors

All volumes located at the sub -volume vertical edges exchange data with diagonal neighbors

3D Configuration: data exchange principle

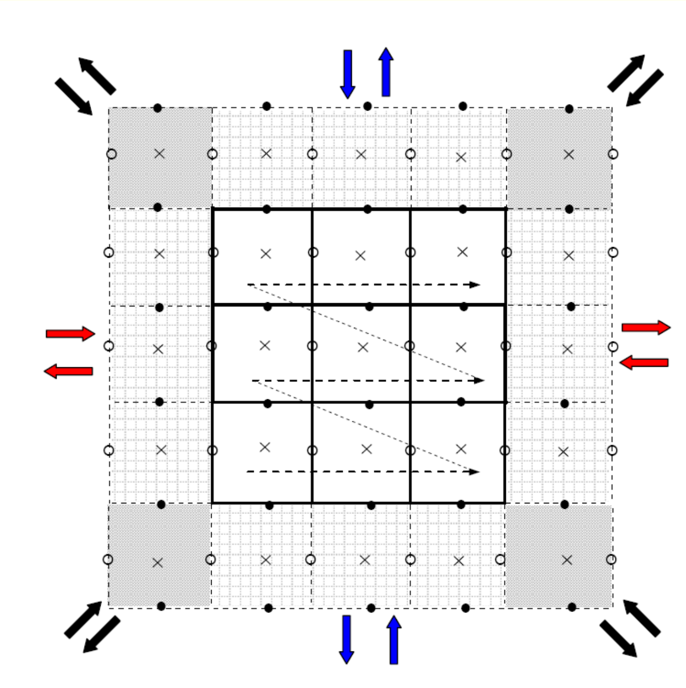

○ v_y velocity

● v_x velocity

x pressure

2 processors overlapping region

4 processors overlapping region

Block relaxation on staggered grid

↓

Simultaneous updating of *i* ,*i*+1 and *j*, *j*+1 velocities

↓

Dependence on velocity values located at the grid points *i* ,*i*±1, *i*±2, *j*, *j*±1, *j*±2

The size of minimal redistributed sub-domain is 3×3

Critical points to enhance algorithm scalability

- **Blocking communication between neighboring processors (synchronous send-and-receive commands) .**
- **Explicit data communication between all neighbor processors , including the diagonal neighbors.**
- **Utilizing telescoping multigrid approach may cause problems in proper balancing on the finest grid, therefore blocking communication should be used.**
- **The decoupled energy equation is solved only on the finest grid by a simple Gauss-Seidel iteration.**

Scalability characteristics of ASA-CLGS - multigrid approach

3D Lid driven cavity, Re=1950: 25^3, 50^3, 100^3 grids

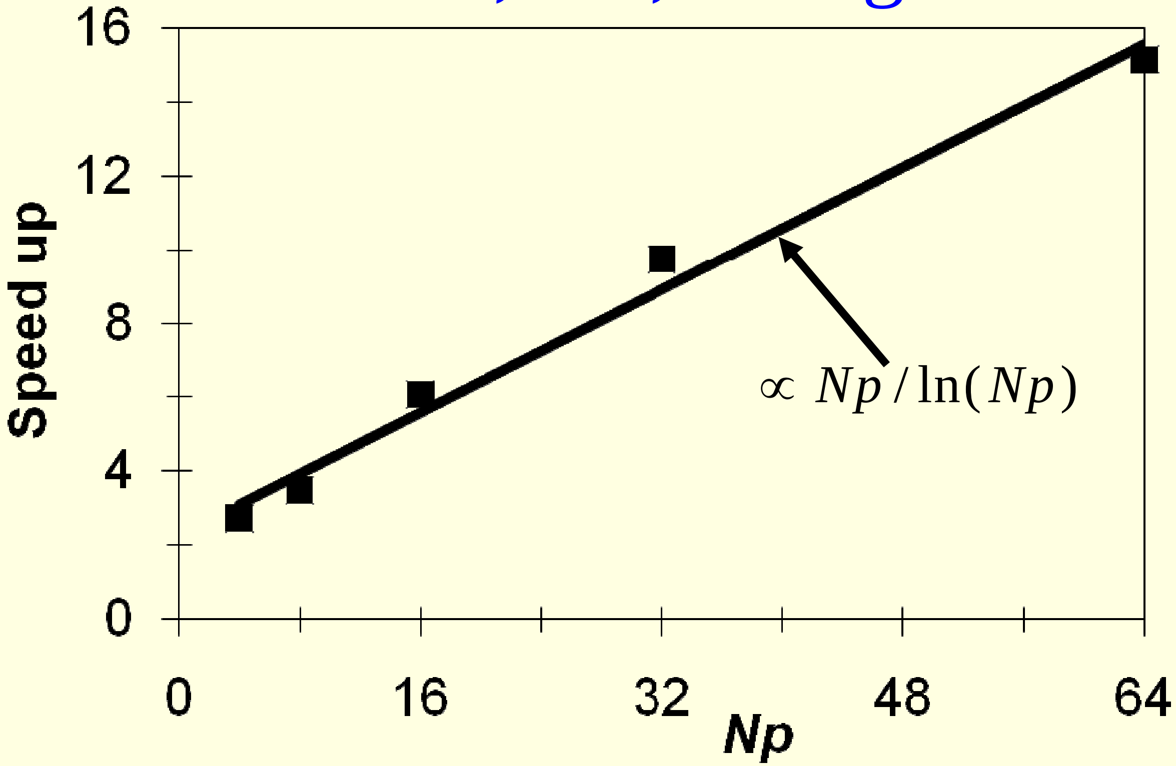

Number of CPU is restricted by the coarsest level (8x8=64 CPU)

Scalability characteristics of ASA-CLGS – single grid approach

3D Lid driven cavity, Re=1950: 200^3 grid

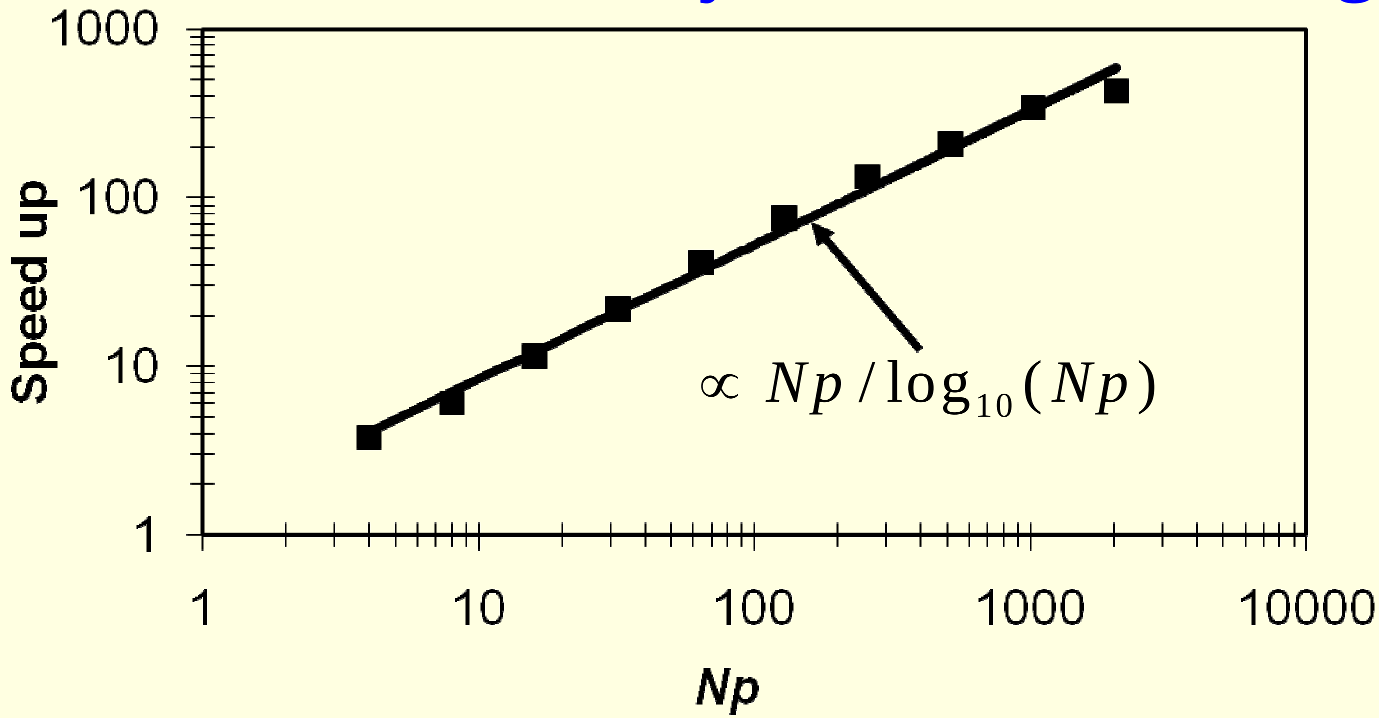

2048 CPU applied on 200^3 grid ➡ 57.4 msec per time step ➡ only 16 hours for 10^6 time steps

General solution strategies

- For a large number of processors the **single-grid** scalability is **significantly more efficient** than that of the multigrid.
- The efficiency of single-grid approach may be obliterated if **at two consecutive time steps** the velocity and/or pressure are **considerably different**. In this case a **relatively low amount** of involved cores will be compensated by a **high convergence rate** of the multigrid.
- Once a stable **asymptotic** regime is approached, the calculations can be performed on the single **finest grid only** with maximal possible number of CPU cores.

Verification: Lid–driven cavity, *Re*=10^3

p, v_y and v_z distribution along two centerlines

The present solution △ and the solution of Albensoeder and Kuhlmann (2005) □

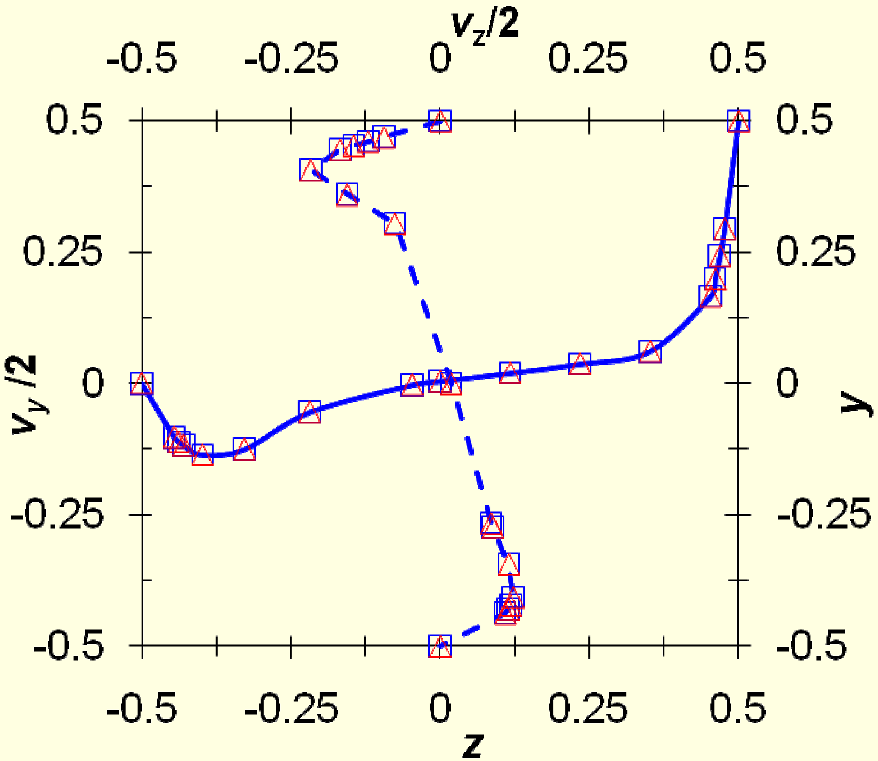

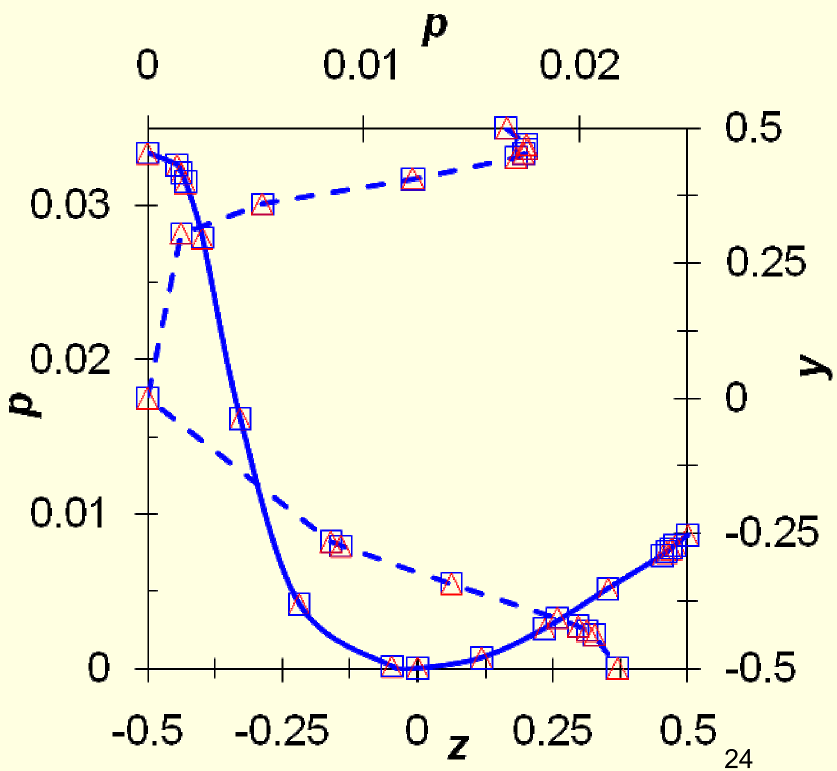

Validation: Lid–driven cavity, $Re=10^3$

Comparison with experiments of A. Liberzon

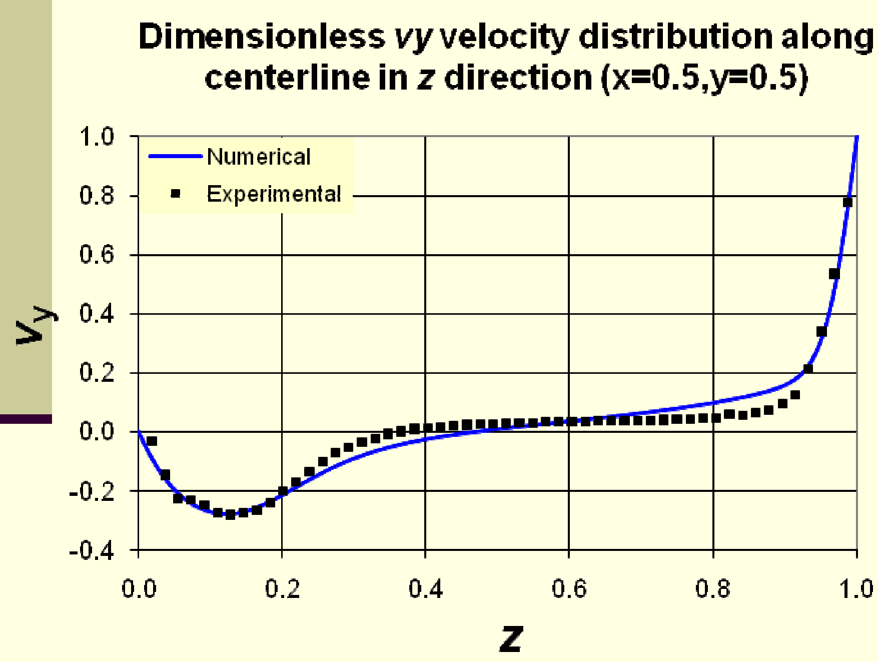

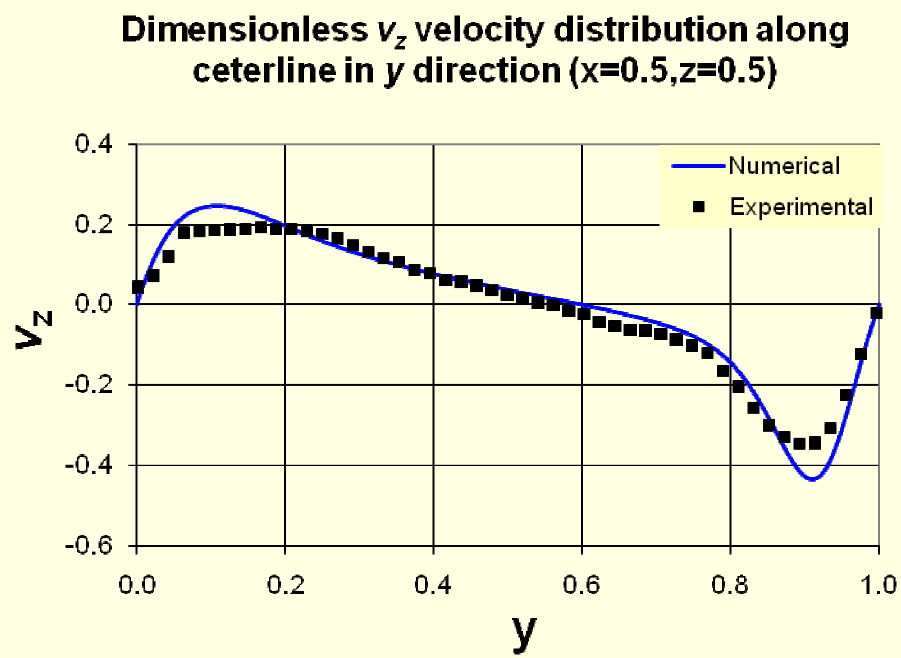

Steady flow in the cubic lid-driven cavity, *Re*=1900

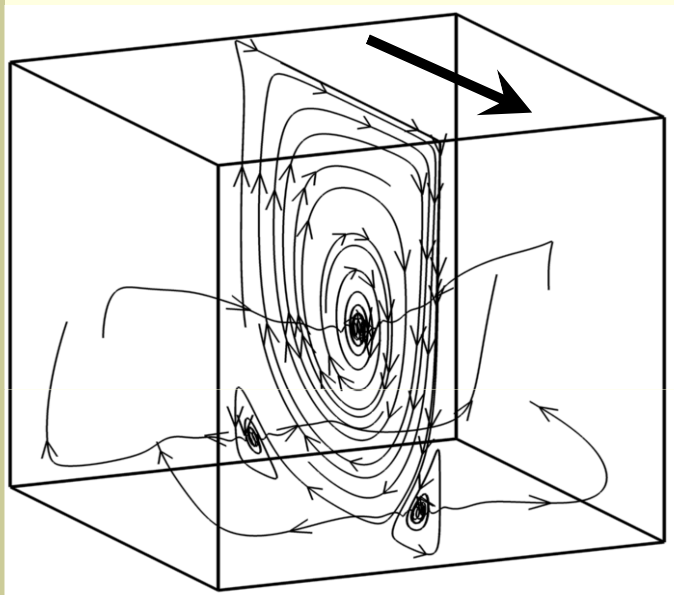

Primary eddy

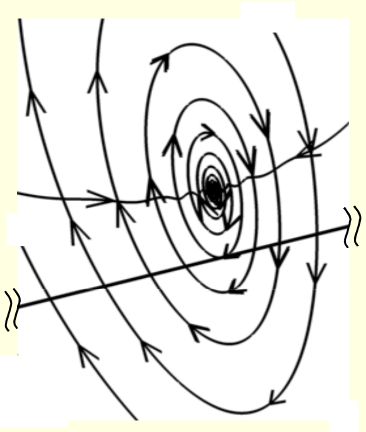

Secondary downstream eddy

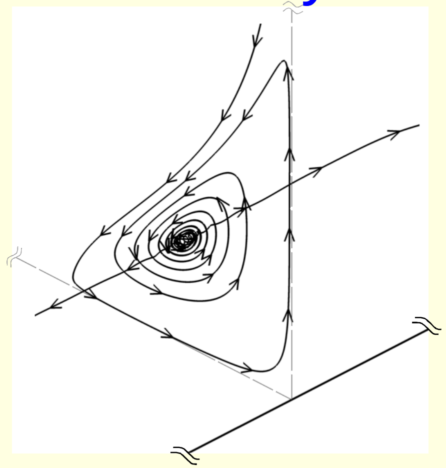

Secondary upstream eddy

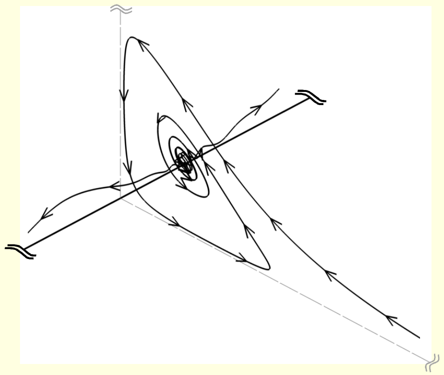

Lid-driven cavity with lid moving at 45° to the *x* axis, *Re*=1000.

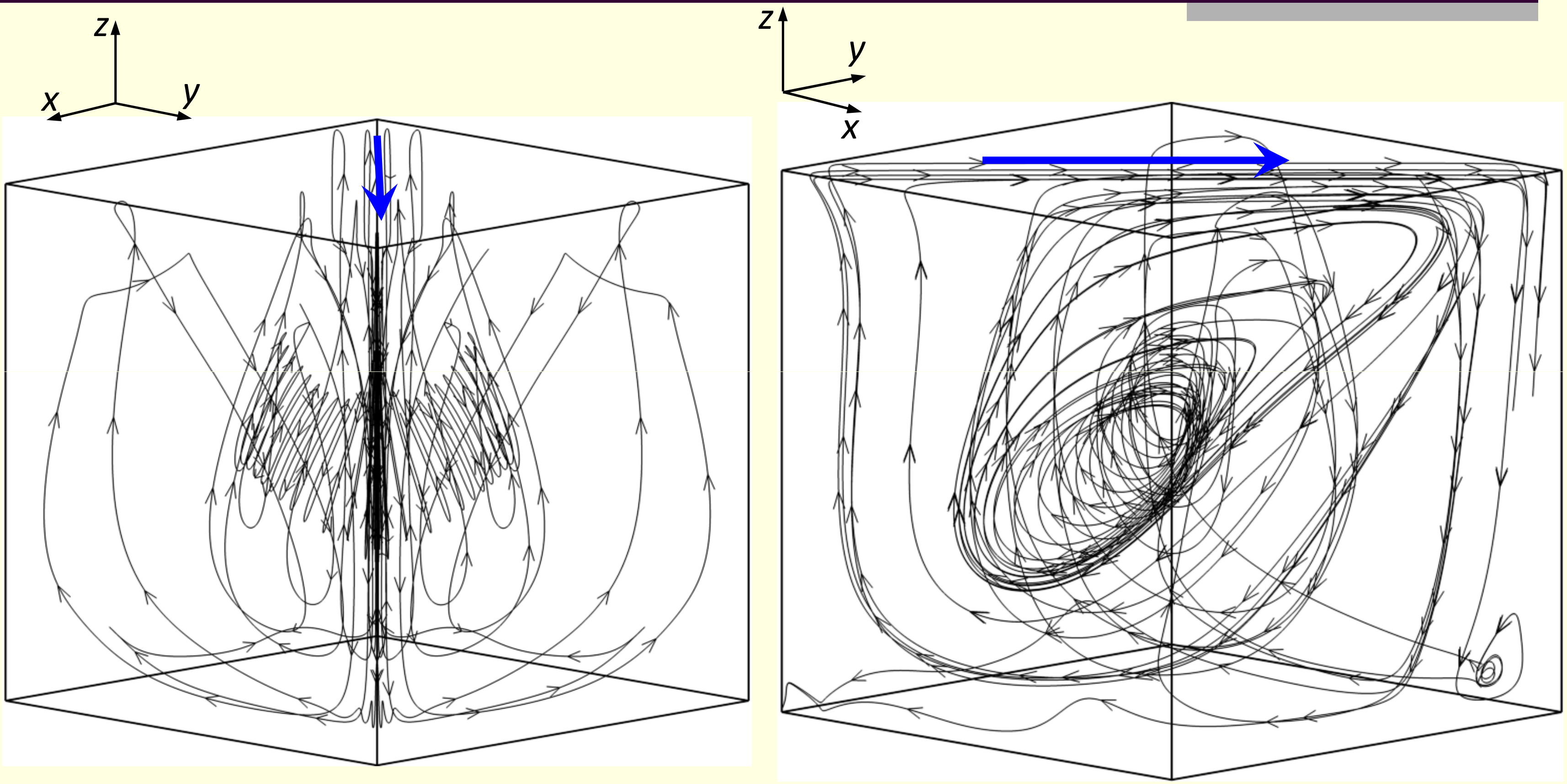

Reflection symmetric flow with respect to diagonal plane

No evidence of the secondary upstream eddy

Oscillatory flow inside cubic lid-driven Cavity, *Re*=1970.

Time evaluation of the total kinetic energy, E_k

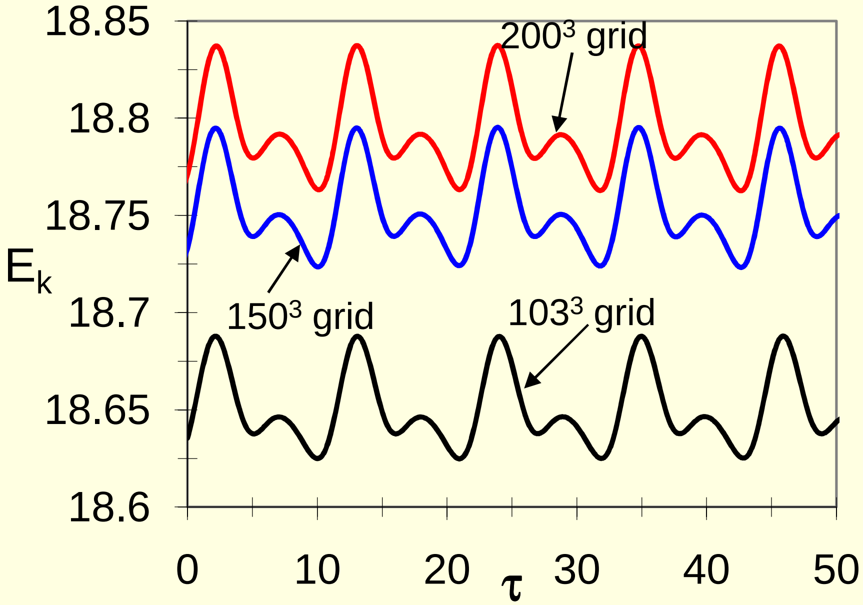

Fourier series of the total kinetic energy, E_k

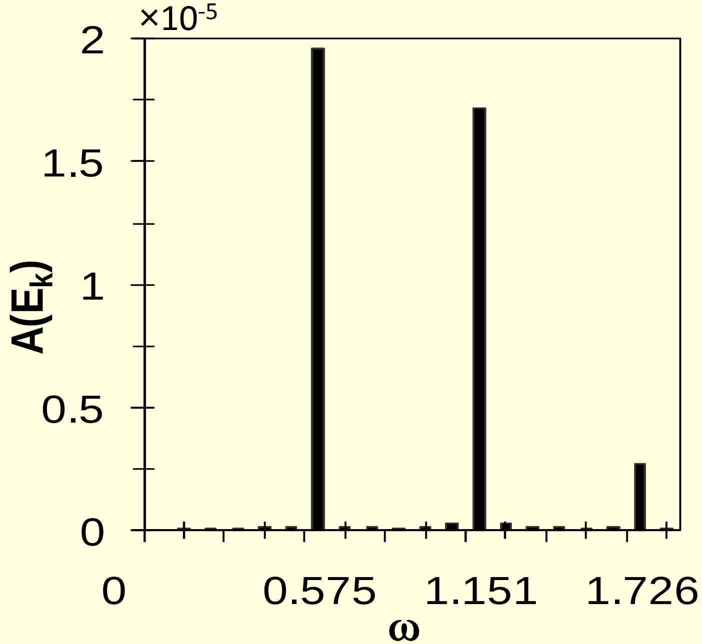

The period of oscillation remains grid-independent

The maximum deviation between the values calculated on 152^3 and 200^3 grids is less then 0.5%.

Oscillatory instability in 2D and 3D lid-driven cavities

2D absolute values of perturbations v'_y and v'_z, *Re*=8700

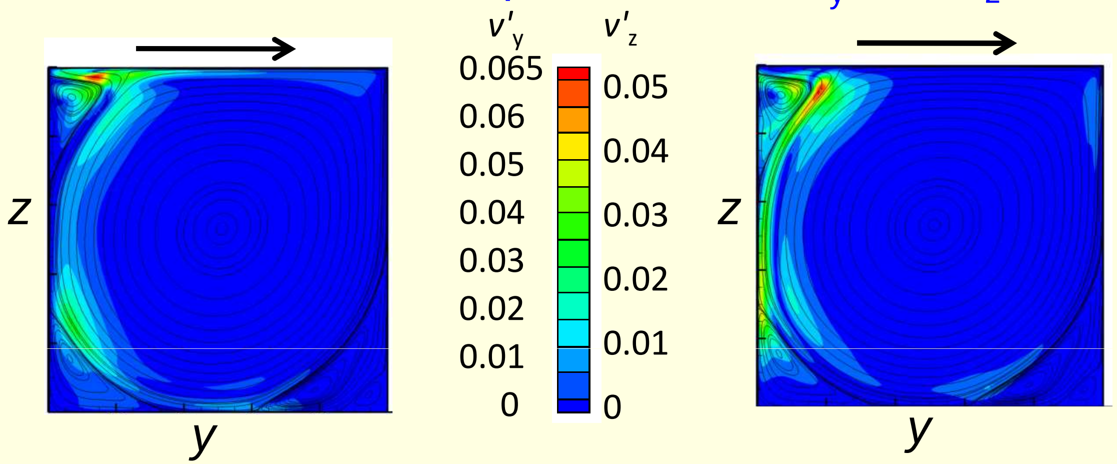

The maximum oscillations for the both perturbations are at the same place

3D v_x and v_z oscillations amplitude at the cavity midplane , *Re*=1970

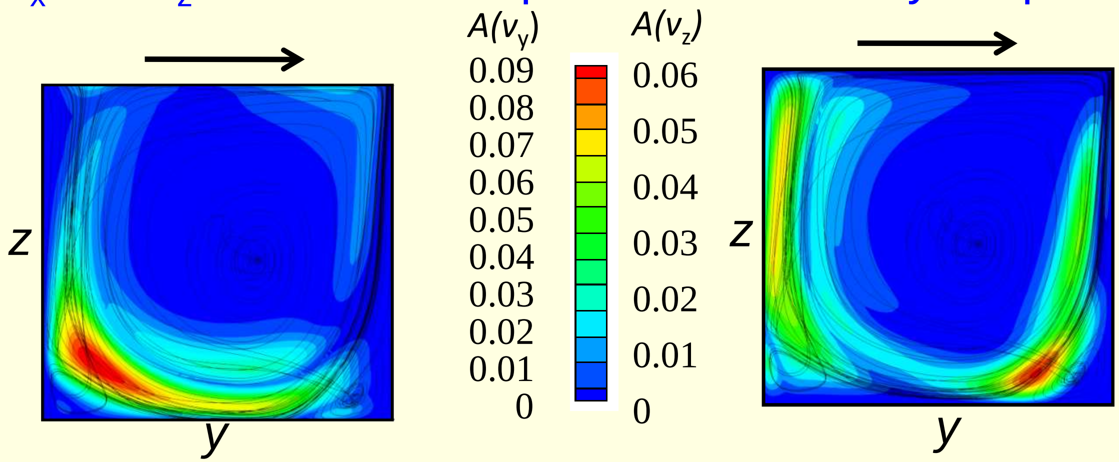

The maximum oscillations for the velocity oscillations are not at the same place

Iso-surface of oscillations amplitude

V_y component

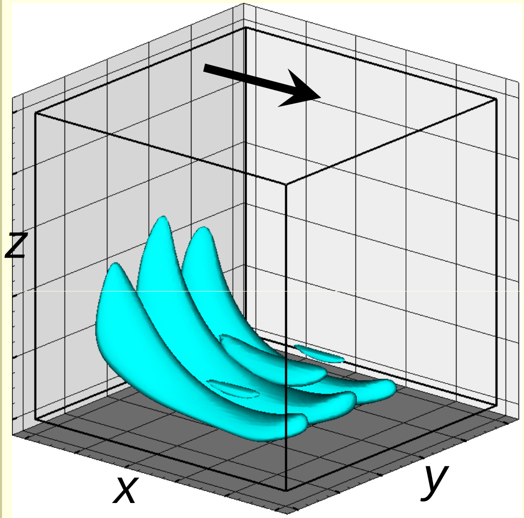

V_z component

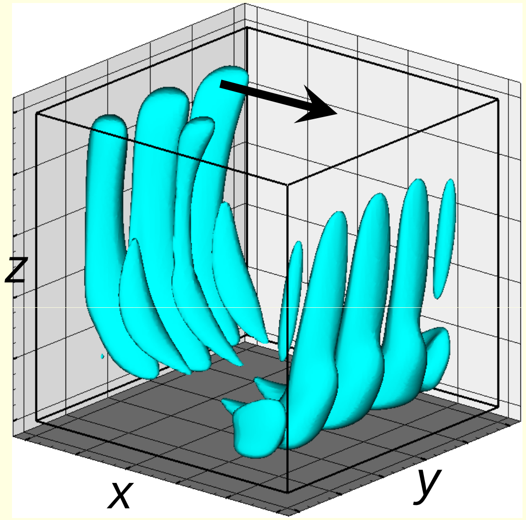

Spanwise V_x component

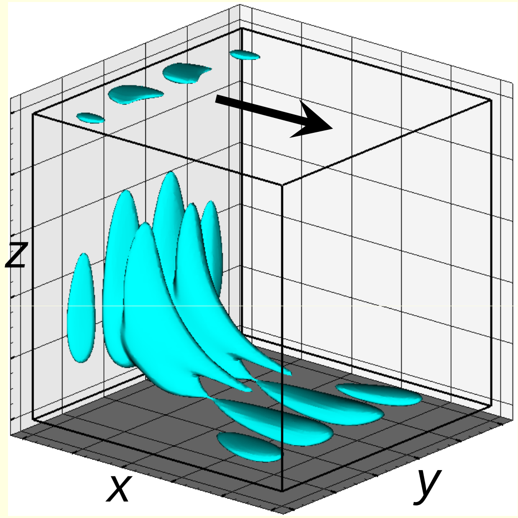

A decay of the amplitudes is observed when approaching the no-slip spanwise boundaries

Subcritical Character of Bifurcation

Oscillations of *x*- and *z*- velocity components at the point (-0.338,-0.338,0)

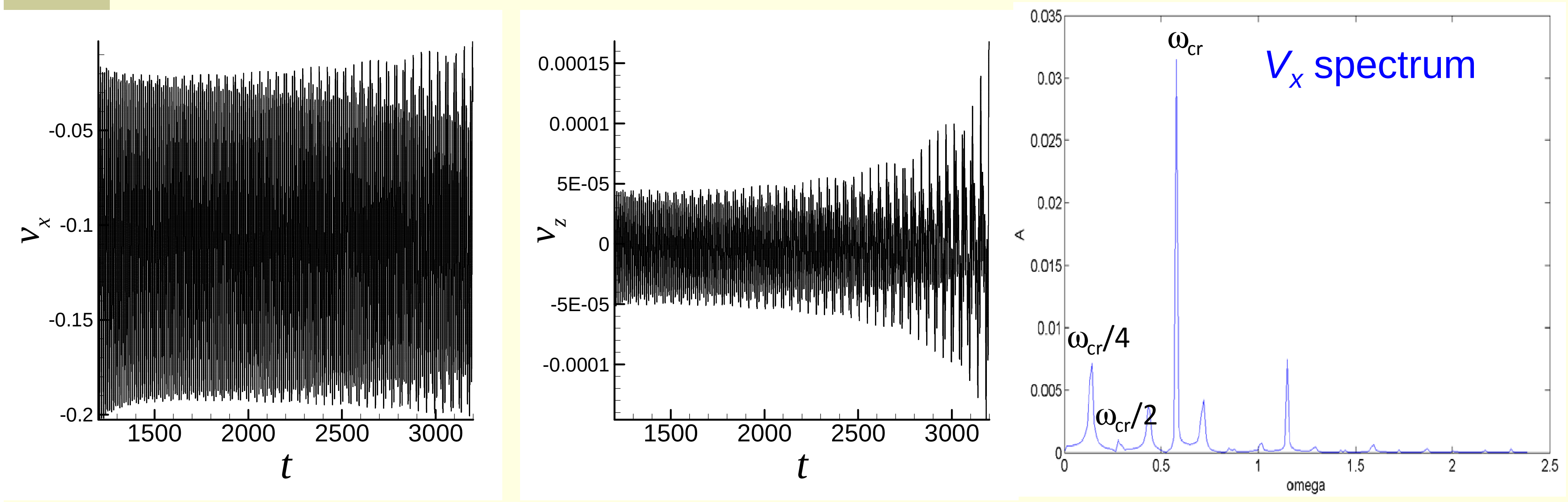

Calculation is preformed on 104^3 grid at *Re*=1945 starting at *t*=0 from oscillatory state at *Re*=1970.

Estimation of Re_{cr} for **subcritical** Hopf bifurcation

Oscillations of *f*(*t*) decay ~ $\exp\left[\left(\lambda_r + i\omega\right)t\right],\ \lambda_r < 0$

$$\lambda_r = \frac{\ln\left(A_k / A_{k-1}\right)}{t_k - t_{k-1}}$$

A_k – *k*-th maximum of an oscillatory signal

Grid Resolution			Re_{cr}	Richardson Extrapolation
104^3	*Re*=1925 $\lambda_r = -3.99\times 10^{-3}$ ω=0.575	*Re*=1955 $\lambda_r = -4.12\times 10^{-4}$ ω=0.575	1958	
152^3	*Re*=1900 $\lambda_r = -4.41\times 10^{-3}$ ω=0.575	*Re*=1925 $\lambda_r = -1.44\times 10^{-3}$ ω=0.575	1937	$Re_{cr}\approx 1919$
200^3	*Re*=1900 $\lambda_r = -3.36\times 10^{-3}$ ω=0.575	*Re*=1925 $\lambda_r = -2.81\times 10^{-4}$ ω=0.575	1927	$Re_{cr}\approx 1914$

Symmetry breaking during the transition from steady to oscillatory flow

Time evolution of v_x component at a point (-0.391,0, 0.395) for *Re*=1970 (solid line), and *Re*=1900 (bold dashed line)

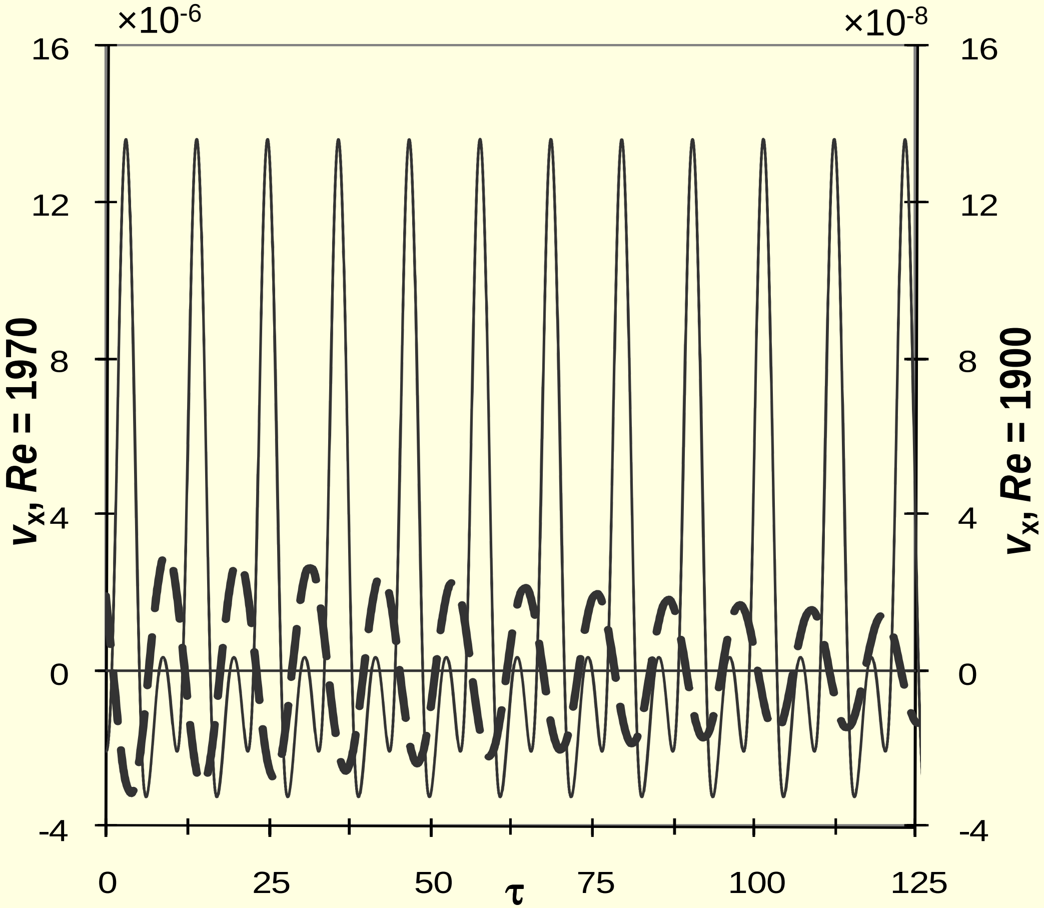

at *Re*=1900, oscillations converge to zero => no flow through the midplane.

non-zero average value of oscillations at *Re*=1970

Maximal v_x and v_y Oscillation Amplitudes at the Cavity Mid-Plane

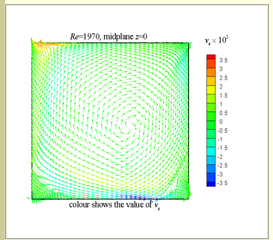

Numerical

v_x Amplitde

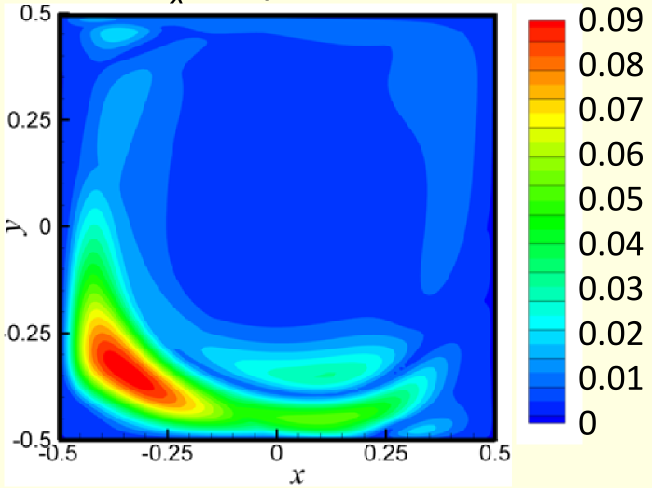

v_y Amplitde

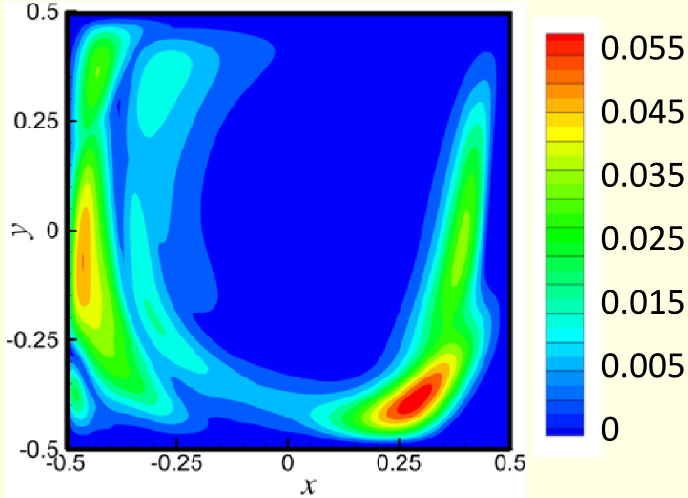

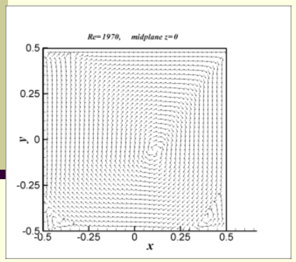

Experimental

v_x Amplitde

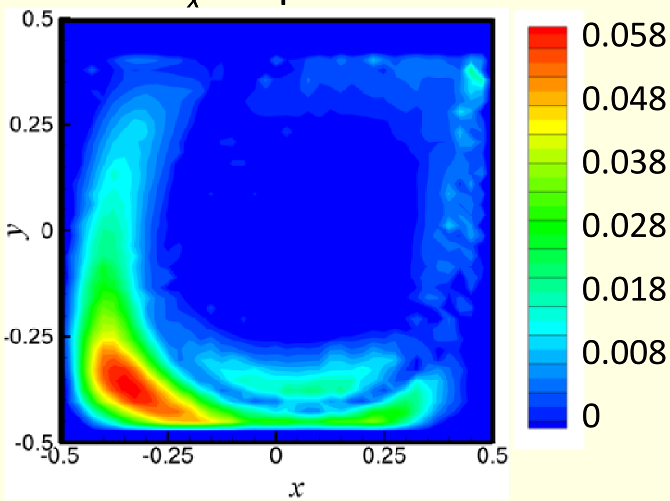

v_y Amplitde

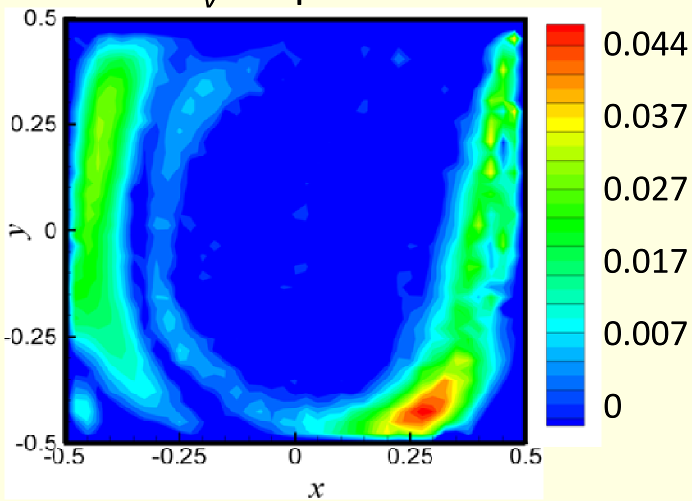

Lid-driven cavity – Summary

- ✓ **Transition from steady to oscillatory state was studied by time-dependent three-dimensional computations on three successive grids of 104^3, 152^3 and 200^3 nodes. Grid independence of the results was established.**
- ✓ **Present time-dependent computations showed that the oscillatory instability of lid driven flow in a cube with no-slip walls takes place at $Re_{cr} \approx 1914$ with a dimensionless frequency $\omega_{cr} = 0.575$.**
- ✓ **The instability sets in via a subcritical Hopf bifurcation.**
- ✓ **The transition from steady to oscillatory state is followed by breaking of the symmetry with respect to the cavity midplane.**

Verification: Differentially heated cavity

Comparison with Wakashima, 2004.
Adiabatic horizontal walls

	Ra=10^4			Ra=10^5			Ra=10^6		
	Wakashima 120^3	Present 100^3	Dev. (%)	Wakashima 120^3	Present 100^3	Dev. (%)	Wakashima 120^3	Present 100^3	Dev. (%)
$u_{y\ max}(z)$ (x=0.5,y=0.5)	0.1984 (0.825)	0.197 (0.825)	**0.7**	0.1416 (0.85)	0.1434 (0.85)	**1.26**	0.0811 (0.8603)	0.0802 (0.8605)	**1.1**
$u_{z\ max}(y)$ (x=0.5,z=0.5)	0.2216 (0.177)	0.2202 (0.12)	**0.6**	0.2464 (0.068)	0.2464 (0.063)	**0**	0.2583 (0.0323)	0.2575 (0.0337)	**0.3**
Nu_{hot}	2.0624	2.0547	**0.37**	4.3665	4.3349	**0.72**	8.6973	8.7584	**0.7**
Nu_{cold}	--------	2.0547	-----	-------	4.3349	-----	---------	8.7584	-----

At the constant *y* plane the average Nu number *is* $\mathrm{Nu}_y = \int_0^1 \int_0^1 \left[\Pr \sqrt{\mathrm{Gr}} V\theta - \frac{\partial \theta}{\partial Y} \right] dX\, dZ$

Steady flow visualization inside the cubic differentially heated cavity

Adiabatic horizontal walls, *Ra*= 10^6

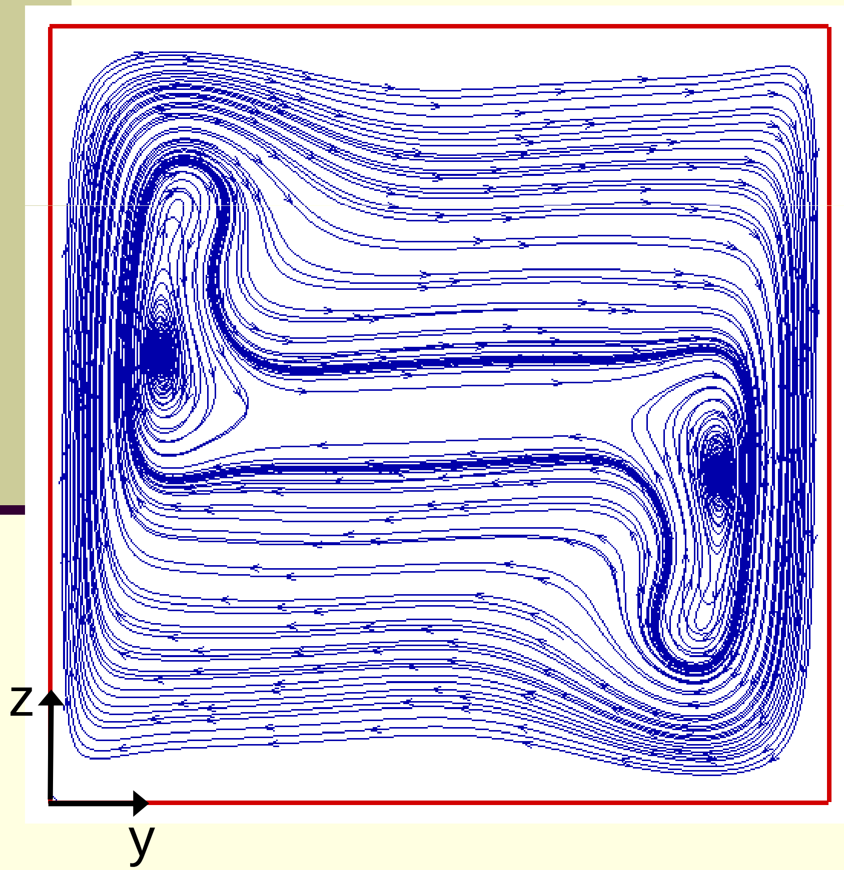

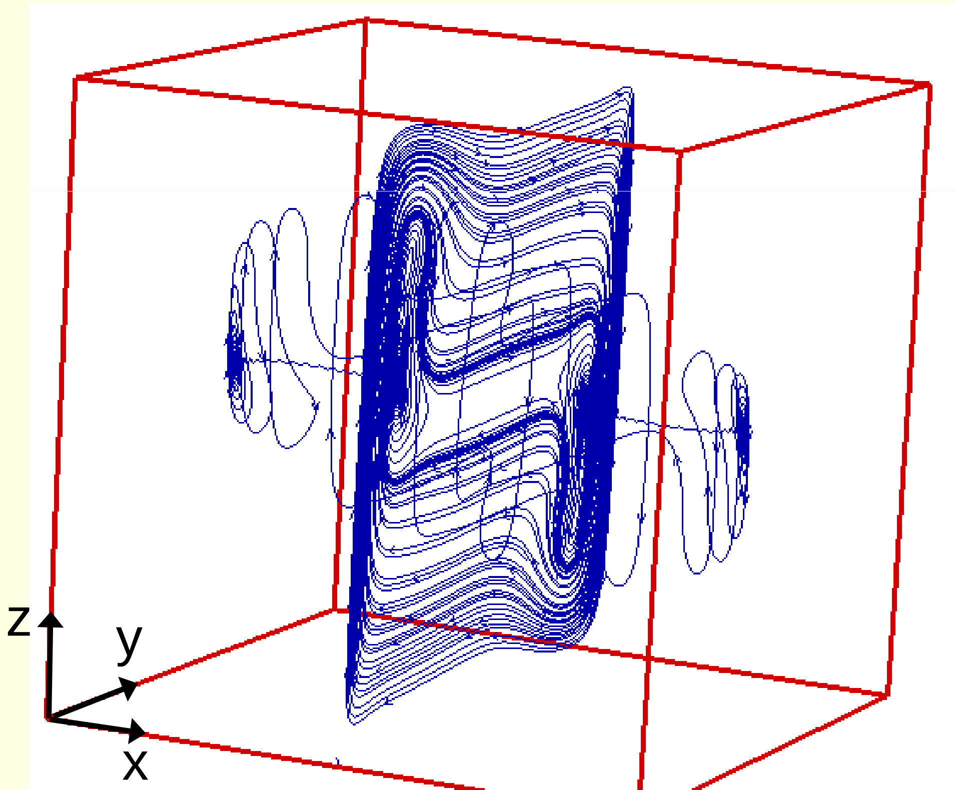

Temperature distribution in a laterally heated cubic cavity

Adiabatic and perfectly conducting horizontal walls, $Ra = 10^6$

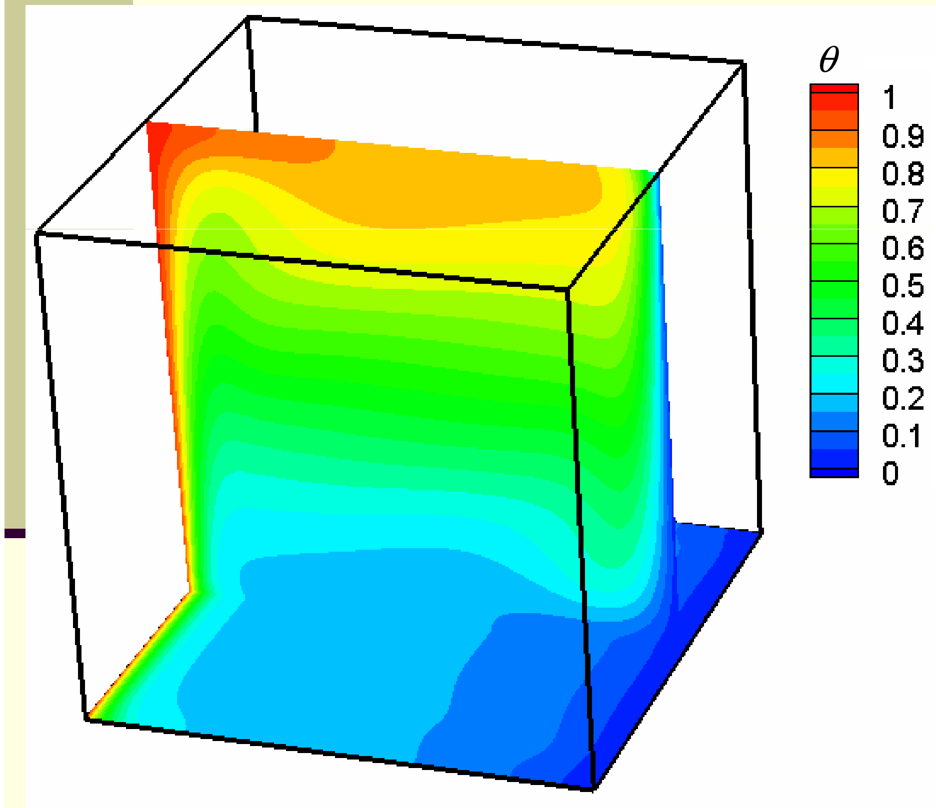

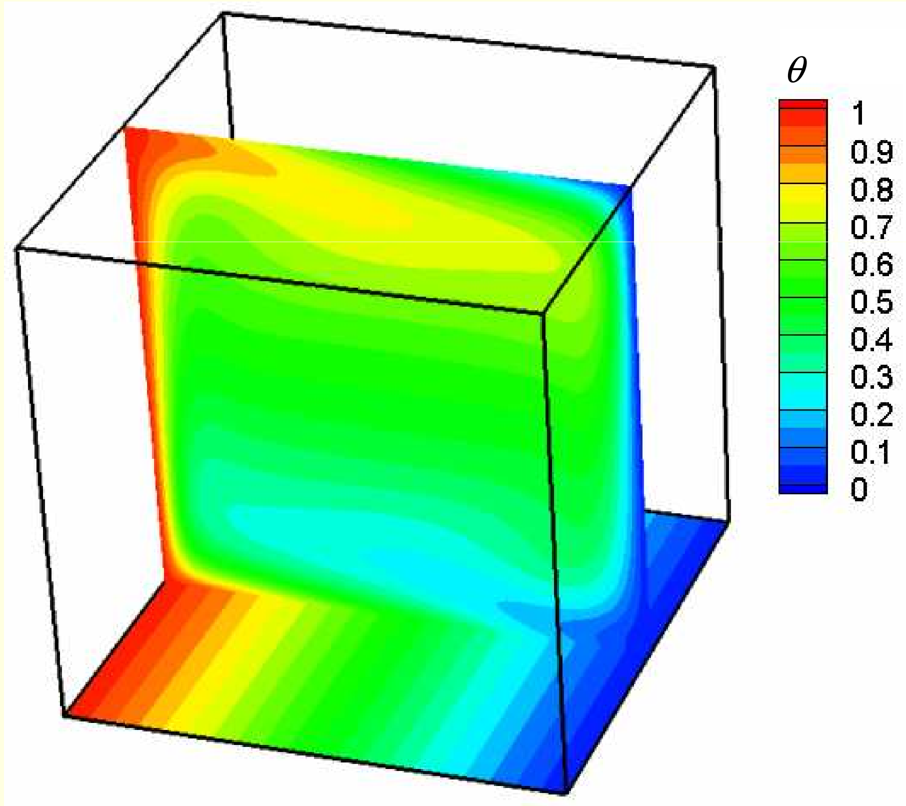

Ra_{cr} for Steady-Oscillatory Transition in a Differentially Heated Cavity, (104^3 grid)

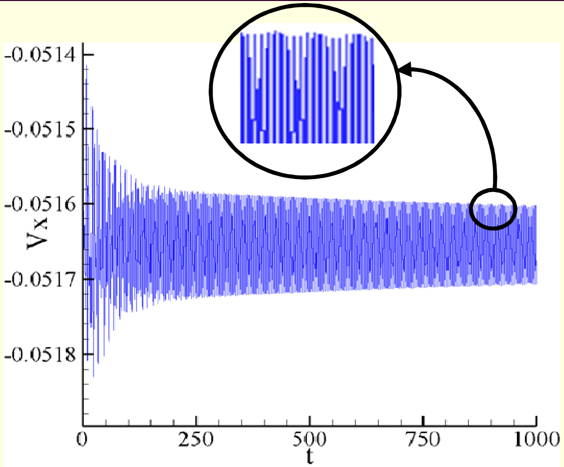

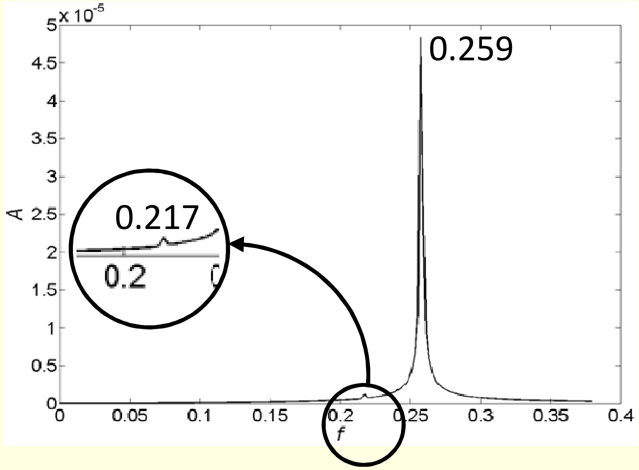

Convergence to Steady Flow

$Ra = 3.05 \times 10^6$

$f = 0.259$

10^6 time steps

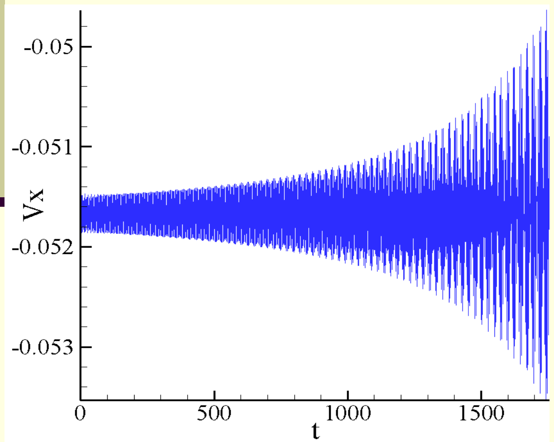

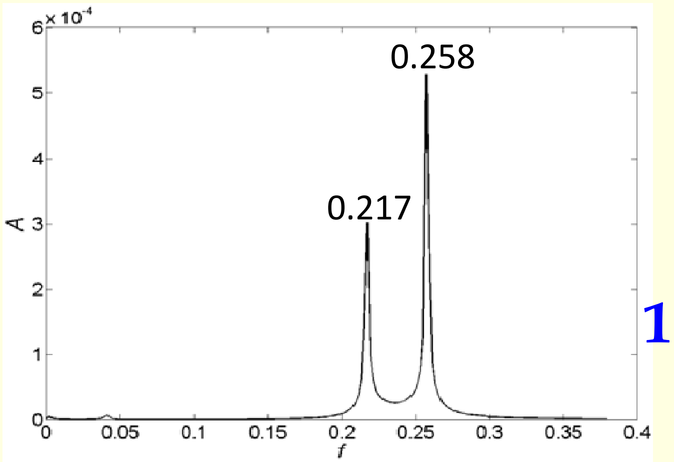

Oscillatory Flow

$Ra = 3.07 \times 10^6$

$f = 0.258$

1.7×10^6 time steps

Experimental Results of Jones and Briggs, 1989 : $f_{cr} \approx 0.248$ $Ra_{cr} \approx 3.0 \times 10^6$

Differentially heated cavity – Summary

- ✓ **The code was successfully verified on existing steady state benchmark solutions for the wide range of *Ra* numbers.**
- ✓ **Preliminary estimation of critical *Gr* number for the Hopf bifurcation on 103^3 grid was performed. The obtained result is well compared with existing experimental data.**
- ✓ **The grid independence should be established by use of finer grids.**

Newton iteration with time-stepping
L.S. Tuckerman, 1999

$$(N_U + L)u = (N + L)U \qquad U \leftarrow U - u$$

$$\underbrace{\left[\left(I - \Delta t L\right)^{-1}\left(I + \Delta t N_U - I\right)\right]}_{\text{Difference between two consecutive linearized time steps}} u = \underbrace{\left[\left(I - \Delta t L\right)^{-1}\left(I + \Delta t N\left(U\right) - I\right)\right]}_{\text{Difference between two consecutive time steps}} U$$

For large Δt, $\left(I - \Delta t L\right)^{-1} \approx L^{-1}$, is a preconditioner for $N_U + L$

Linear stability analysis with time-stepping
L.S. Tuckerman, 1999

Inverse power method for the leading eigen value

$$u_{n+1} = \left(N_U + L\right)^{-1} u_n$$

$$\underbrace{\left[\left(I - \Delta t L\right)^{-1}\left(I + \Delta t N_U - I\right)\right]}u_{n+1} = \underbrace{\left(I - \Delta t L\right)^{-1}}\Delta t u_n$$

Difference between two consecutive linearized time steps

Difference between two consecutive time steps of the Stokes operator

Good performance for 2D configuration

Still a challenge for 3D configuration

Conclusions

- A novel multigrid solver for time-dependent incompressible Navier-Stokes equations in pressure-velocity coupled formulation is developed and implemented.
- The characteristic CPU times consumed for a single time step per one node and per one CPU are of order 5×10^{-3} msec and 10^{-2} msec for 2D and 3D calculations, respectively.
- The approach performs well for time-dependent calculations with a small time step,
- Direct Newton and Arnoldi iterations needed for stability analysis require large time steps, which causes a slow convergence for 3D problems